

Revised Effective Ionic Radii and Systematic Studies of Interatomic Distances in Halides and Chalcogenides

BY R. D. SHANNON

Central Research and Development Department, Experimental Station, E. I. Du Pont de Nemours and Company, Wilmington, Delaware 19898, U.S.A.

(Received 30 October 1975; accepted 9 March 1976)

The effective ionic radii of Shannon & Prewitt [Acta Cryst. (1969), B25, 925–945] are revised to include more unusual oxidation states and coordinations. Revisions are based on new structural data, empirical bond strength–bond length relationships, and plots of (1) radii *vs* volume, (2) radii *vs* coordination number, and (3) radii *vs* oxidation state. Factors which affect radii additivity are polyhedral distortion, partial occupancy of cation sites, covalence, and metallic character. Mean Nb⁵⁺–O and Mo⁶⁺–O octahedral distances are linearly dependent on distortion. A decrease in cation occupancy increases mean Li⁺–O, Na⁺–O, and Ag⁺–O distances in a predictable manner. Covalence strongly shortens Fe²⁺–X, Co²⁺–X, Ni²⁺–X, Mn²⁺–X, Cu⁺–X, Ag⁺–X, and M–H[–] bonds as the electronegativity of X or M decreases. Smaller effects are seen for Zn²⁺–X, Cd²⁺–X, In³⁺–X, Pb²⁺–X, and Tl⁺–X. Bonds with delocalized electrons and therefore metallic character, *e.g.* Sm–S, V–S, and Re–O, are significantly shorter than similar bonds with localized electrons.

Introduction

A thorough and systematic knowledge of the relative sizes of ions in halides and chalcogenides is rapidly being developed by crystal chemists as a result of (1) extensive synthesis within certain structure types, *e.g.* rocksalt, spinel, perovskite and pyrochlore; (2) preparation of new compounds with unusual oxidation states and coordination numbers; and (3) the abundance of accurate crystal structure refinements of halides, chalcogenides, and molecular inorganic compounds. A set of effective ionic radii which showed a number of systematic trends with valence, electronic spin state, and coordination was recently developed (Shannon & Prewitt, 1969, hereafter referred to as SP 69). This work has since been supplemented and improved by studies of certain groups of ions: rare earth and actinide ions (Peterson & Cunningham, 1967, 1968); tetrahedral oxyanions (Kálmán, 1971); tetravalent ions in perovskites (Fukunaga & Fujita, 1973); rare earth ions (Greis & Petzel, 1974); and tetravalent cations (Knop & Carlow, 1974).

Further, the relative sizes of certain ions or ion pairs were studied by Khan & Baur (1972): NH₄⁺; Ribbe & Gibbs (1971): OH[–]; Wolfe & Newnham (1969): Bi³⁺–La³⁺; McCarthy (1971): Eu²⁺–Sr²⁺; Silva, McDowell, Keller & Tarrant (1974): No²⁺. These authors' results have been incorporated here into a comprehensive modification of the Shannon–Prewitt radii.

In this paper the revised list of effective ionic radii, along with the relations between radii, coordination number, and valence is presented. The factors responsible for the deviation of radii sums from additivity such as polyhedral distortion, partial occupancy of cation sites, covalence, and metallic behavior (electron delocalization) will be discussed.

Procedure

The same basic methods used in SP 69 were employed in preparing the revised list of effective ionic radii (Table 1). Some of the same assumptions were made:

(1) Additivity of both cation and anion radii to reproduce interatomic distances is valid if one considers coordination number (CN), electronic spin, covalency, repulsive forces, and polyhedral distortion.*

(2) With these limitations, radii are independent of structure type.

(3) Both cation and anion radii vary with coordination number.

(4) With a constant anion, unit-cell volumes of isostructural series are proportional (but not necessarily linearly) to the cation volumes.

Other assumptions made in SP 69 have been modified:

(1) The effects of covalency on the shortening of M–F and M–O bonds are *not* comparable.

(2) Average interatomic distances in similar polyhedra in one structure are *not* constant but vary in a predictable way with the degree of polyhedral distortion (and anion CN). Both of these modified assumptions will be discussed in detail later.

The anion radii used in SP 69 were subtracted from available average distances. Approximately 900 distances from oxide and fluoride structures were used, and Table 2 lists their references according to CN and spin. These references generally cover from 1969 to 1975. The cation radii were derived to a first approximation from these distances, and then adjusted to be consistent with both the experimental interatomic distances and radii–unit cell volume (*r*³ *vs* *V*) plots, as in

* Polyhedral distortion was not considered in SP 69.

compounds to be slightly larger than those of the Eu^{2+} compounds. This difference was assumed to exist for all Sr^{2+} and Eu^{2+} coordinations. Because compounds of Am^{2+} and Sr^{2+} have similar cell volumes, the radius of Am^{2+} was made equal to that of Sr^{2+} .

Wolfe & Newnham (1969) studied $\text{Bi}_{4-x}\text{RE}_x\text{Ti}_3\text{O}_{12}$ and concluded that Bi^{3+} and La^{3+} have nearly equal radii. From a study of BiTaO_4 Sleight & Jones (1975) have concluded that although Bi^{3+} and La^{3+} have essentially equal radii, the size of Bi^{3+} depends on the degree of the $6s^2$ lone-pair character. When BiTaO_4 transforms from a structure where the lone-pair character is dominant to the LaTaO_4 structure, it undergoes a volume reduction. Table 3 shows a comparison of isotopic Bi^{3+} and La^{3+} compounds where the lone-pair character of Bi^{3+} is (1) constrained and (2) dominant. Bi pyrochlores such as $\text{Bi}_2\text{Ru}_2\text{O}_7$, $\text{Bi}_2\text{Ir}_2\text{O}_7$ and $\text{Bi}_2\text{Pt}_2\text{O}_7$ were omitted from the table because no corresponding La pyrochlore exists, but they have unit-cell volumes close to those of the Sm or Nd pyrochlores and thus have smaller volumes than those of La. When Bi^{3+} is forced into high symmetry, a Bi^{3+} compound has a smaller volume than that of La^{3+} , but when the lone-pair character is dominant, the Bi^{3+} compound is distorted and Bi^{3+} and La^{3+} compounds have approximately equal volumes. This behavior was also noted in the highly symmetric garnet structure where the hypothetical $\text{Bi}_3\text{Fe}_3\text{O}_{12}$ was estimated to have cell dimensions between those of the hypothetical $\text{Nd}_3\text{Fe}_3\text{O}_{12}$ and $\text{Pr}_3\text{Fe}_3\text{O}_{12}$ (Geller, Williams, Espinosa, Sherwood & Gilleo, 1963). For practical purposes, Bi^{3+} is listed as slightly smaller than La^{3+} but this dependence on lone-pair character must be kept in mind when comparing the volumes of Bi^{3+} and La^{3+} compounds. Similar behavior may also exist for Pb^{2+} and Sr^{2+} , but this relationship was not investigated.

Table 3. Cell volumes of isotopic Bi^{3+} and La^{3+} compounds

(a) Lone pair character of Bi^{3+} constrained

Compound	Cell volume	Ratio
$\text{BiLi}(\text{MoO}_4)_2$	314.7	0.96
$\text{LaLi}(\text{MoO}_4)_2$	328.7	
$\text{BiNa}(\text{MoO}_4)_2$	320.5	0.97
$\text{LaNa}(\text{MoO}_4)_2$	332.1	
BiOF	87.6	0.90
LaOF	97.7	
BiOCl	110.7	0.95
LaOCl	116.8	
BiOBr	123.8	0.98
LaOBr	126.4	
BiPO_4	293.0	0.96
LaPO_4	304.7	

(b) Lone pair character of Bi^{3+} dominant

Bi_2MoO_6	268.5 ($\times 8$)	1.00
La_2MoO_6	267.3	
BiFeO_3	62.49 ($\times 6$)	1.03
LaFeO_3	60.77 ($\times 4$)	
$\text{Bi}_2\text{Sn}_2\text{O}_7$	1219.9 ($\times 8$)	1.00
$\text{La}_2\text{Sn}_2\text{O}_7$	1225.3	

A similar study of relative cell volumes of isotopic compounds involving the pairs $\text{Cu}^+\text{-Li}^+$, $\text{Ag}^+\text{-Na}^+$, $\text{Tl}^+\text{-Rb}^+$, and $\text{Pb}^{2+}\text{-Sr}^{2+}$ was used to obtain more reliable estimates of the radii of Cu^+ , Ag^+ , Tl^+ , and Pb^{2+} (Shannon & Gumerman, 1975).

The nature of Sn^{2+} , NH_4^+ , and H^- made it impossible to define their ionic radii. The coordination of Sn^{2+} by oxygen or fluorine is always extremely irregular,* leading to average distances which depend on the degree of distortion. Since this distortion varies widely from one compound to another, it is not meaningful to define an ionic radius.

Khan & Baur (1972) derived an apparent radius of the NH_4^+ ion by analyzing the N-O distances in a large number of ammonium salts. They concluded that NH_4^+ has an octahedral radius of 1.61 Å, between that of Rb^+ (1.52 Å) and Cs^+ (1.67 Å). Alternatively, cell volumes of NH_4^+ and Rb^+ fluorides, chlorides, bromides, iodides and oxides may be compared. This leads to the conclusion that NH_4^+ is not significantly different in size from Rb^+ . No explanation is offered for this inconsistency and therefore the radius of NH_4^+ is not included.

The radius of the hydride ion, H^- , has been the subject of some controversy. A number of different radii have been proposed: 2.08 (Pauling, 1960); 1.40 (Gibb, 1962); and 1.53 Å (Morris & Reed, 1965). Gibb studied interatomic distances in many hydrides and concluded that good agreement between observed and calculated distances could be obtained using $r(\text{VIH}^-) = 1.40$ Å if corrected for cation and anion coordination. The value of $r(\text{IVH}^-)$ was taken to be 1.22 Å.

Morris & Reed (1965) concluded that differences in observed distances in hydrides were caused by the large H^- polarizability. Because of such wide variations in the apparent H^- radius, it was omitted. However, an explanation for the variations based on covalence differences will be discussed later.

* Although cell dimensions of $\text{Sn}_2\text{M}_2\text{O}_7$ pyrochlores were used in SP 69 to derive $r(\text{VIISn}^{2+})$, Stewart, Knop, Meads & Parker (1973) and Birchall & Sleight (1975) recently found that the pyrochlore A site in $\text{Sn}_2\text{Ta}_2\text{O}_7$ is not fully occupied. Thus, even this example of apparently regular Sn^{2+} polyhedra is not valid.

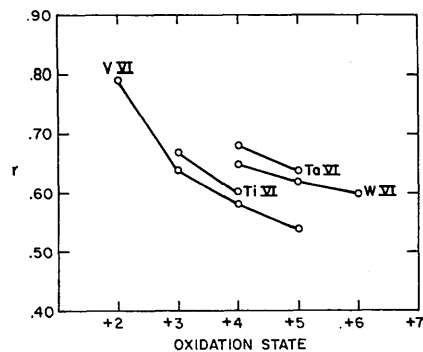
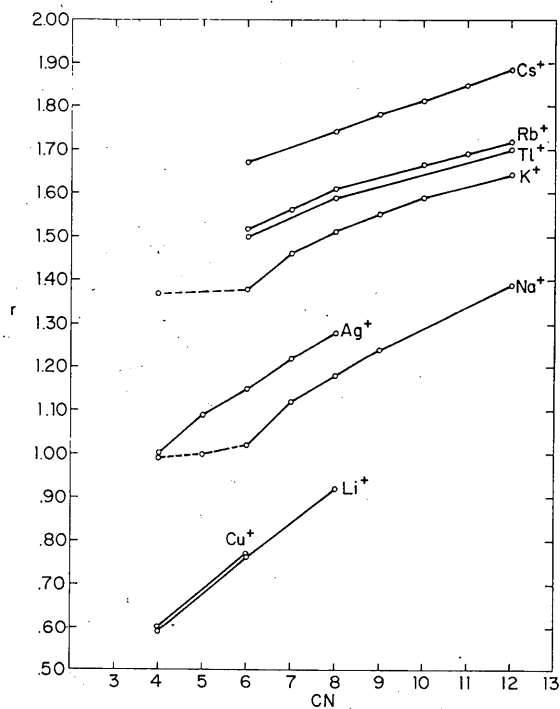


Fig. 1. Effective ionic radius (Å) vs oxidation state.

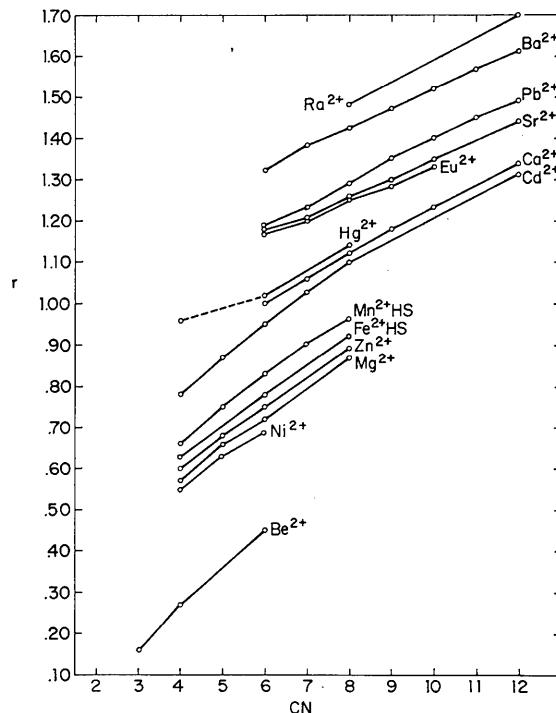
Results and discussion

In Table 1 two sets of radii are included. The first is a set of traditional radii based on $r(\text{VI}\text{O}^{2-}) = 1.40 \text{ \AA}$. The

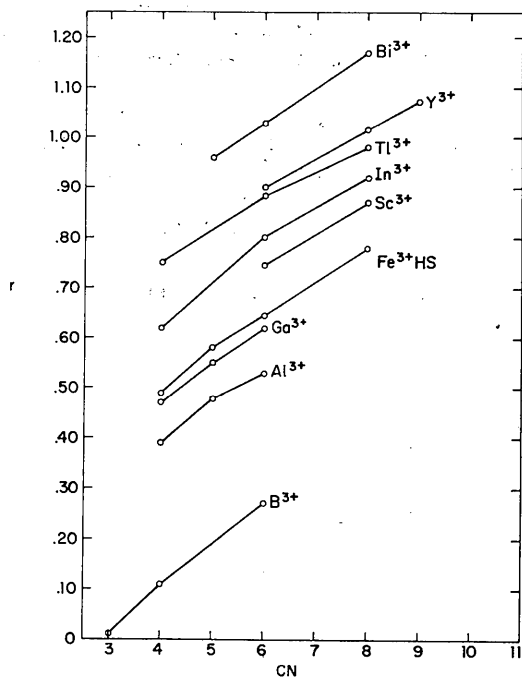
other set is based on $r(\text{VI}\text{O}^{2-}) = 1.26$ and $r(\text{VI}\text{F}^-) = 1.19 \text{ \AA}$, and corresponds to crystal radii as defined by Fumi & Tosi (1964). As pointed out in SP 69, crystal radii differ from traditional radii only by a constant factor



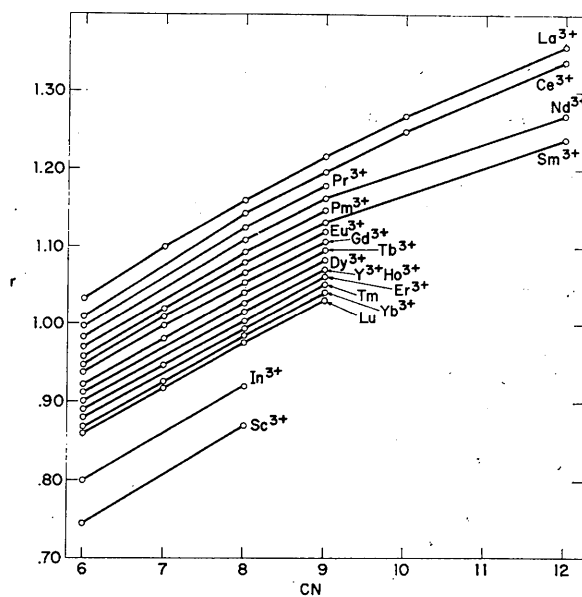
(a)



(b)

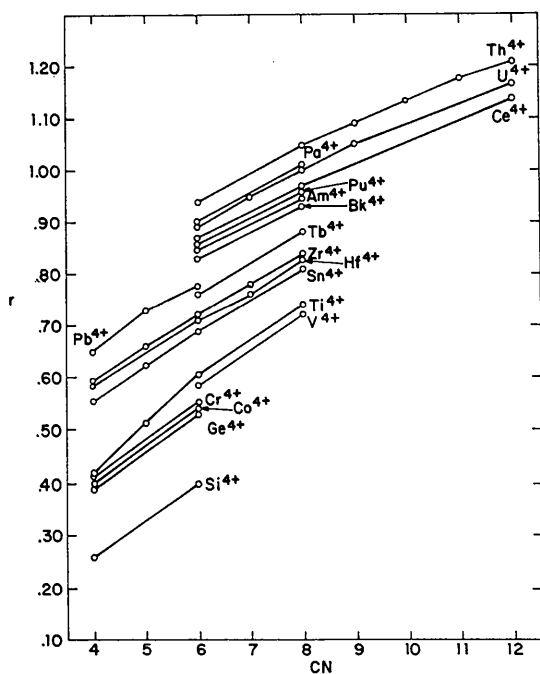


(c)



(d)

Fig. 2. (a)–(e) Effective ionic radius (Å) vs CN for some common cations.



(e)

Fig. 2. (cont.)

of 0.14 Å. Although their inclusion in Table 1 may seem superfluous, it is felt that crystal radii correspond more closely to the physical size of ions in a solid. They should be used, for example, in discussions of closest packing of spheres, structure field maps (Muller & Roy, 1974), and diffusion in solids (Flygare & Huggins, 1973). Traditional radii have been retained because of their familiarity to crystal chemists and physicists. They will probably continue to be used for comparison of unit-cell volumes and interatomic distances. In the table, the ion is followed by electron configuration (EC), coordination number (CN), spin state (SP), crystal radius (CR), and effective ionic radius (IR), and in the last column, a symbol indicating the derivation of the radii and their reliability. Those with a question mark are doubtful because of: uncertainty in CN, or deviation from radii *vs* CN, or radii *vs* valence plots. Where at least five structural determinations resulted in radii differing by no more than ± 0.01 Å, the values are marked with an asterisk.

When the choice of a radius was influenced by any of the various correlations described earlier, it is indicated by the following: *R* – from r^3 *vs* unit cell volume plots; *C* – calculated from bond length–bond strength equations; *E* – estimated from one or more plots of *r vs* valence, *r vs* CN, and *r vs* cell volume. *E* implies poor or nonexistent structural data. Radii in this category include ${}^{\text{VI}}\text{Fe}^{2+}\text{LS}$, ${}^{\text{VI}}\text{Mn}^{2+}\text{LS}$, ${}^{\text{VI}}\text{Cr}^{2+}\text{LS}$, ${}^{\text{VI}}\text{V}^{2+}$, ${}^{\text{VI}}\text{Ni}^{3+}\text{HS}$, ${}^{\text{VI}}\text{Ir}^{3+}$, ${}^{\text{VI}}\text{Mo}^{3+}$, ${}^{\text{VI}}\text{Ta}^{3+}$, ${}^{\text{VI}}\text{Pa}^{3+}$, ${}^{\text{VI}}\text{Ta}^{4+}$, ${}^{\text{IV}}\text{Pb}^{4+}$, ${}^{\text{VI}}\text{Ir}^{5+}$, ${}^{\text{VI}}\text{Os}^{5+}$, ${}^{\text{VI}}\text{Re}^{5+}$, ${}^{\text{VI}}\text{Pu}^{5+}$, ${}^{\text{VI}}\text{Bi}^{5+}$,

${}^{\text{VI}}\text{Os}^{6+}$, ${}^{\text{VI}}\text{Re}^{6+}$, and ${}^{\text{VI}}\text{Os}^{7+}$. The symbol *A* means that Ahrens (1952) ionic radius was used whereas *P* means Pauling's (1960) crystal radius was used. The symbol *M* means that the radius was derived from a compound having metallic conductivity. Distances calculated from these radii may be too small for use in compounds having localized electrons. (See discussion *Effects of electron delocalization*.)

In addition, the sources of the radii are indicated in Table 2.

Fig. 2(a)–(e) shows that *r*–CN plots are reasonably regular. Notable exceptions are ${}^{\text{IV}}\text{Na}^+$, ${}^{\text{V}}\text{Na}^+$, and ${}^{\text{IV}}\text{K}^+$. It is apparent that Na–O and K–O distances do not decrease as much as anticipated from the *r*–CN curve* when the CN falls below six. Typical distances and corresponding radii in Table 4 show that Na–O distances in four-coordination are only slightly less than in six-coordination. The reduction in interatomic distances is caused primarily by the decreased repulsive forces due to fewer ligands according to the expression of Pauling (1960):

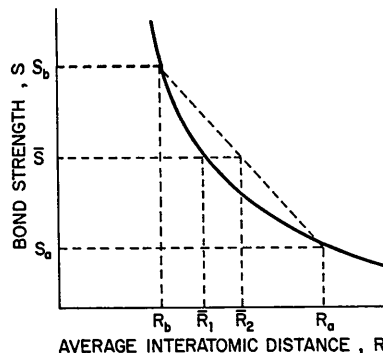
$$\frac{R_{\text{CsCl}}}{R_{\text{NaCl}}} = \left[\frac{A_{\text{NaCl}}}{A_{\text{CsCl}}} \frac{B_{\text{CsCl}}}{B_{\text{NaCl}}} \right]^{1/(n-1)}$$

where *R* = interatomic distance, *A* = Madelung constant, *B* = the cation CN and *n* = Born repulsion coefficient. It appears that this equation is not valid for four-coordinated Na^+ or K^+ .

There are a few small irregularities in *r*–CN plots probably caused by poor or insufficient data, e.g. curves for Ti^{3+} *vs* Y^{3+} . The differences in slopes of Ti^{4+} *vs* Cr^{4+} and V^{5+} *vs* As^{5+} are probably caused by Ti^{4+} –O and V^{5+} –O octahedra being generally more distorted, which leads to greater average interatomic distances.

It is also interesting to compare distances in square planar coordination *versus* tetrahedral coordination. Radii of square planar Cu^{2+} and Ag^+ are equal to or slightly greater than corresponding tetrahedral radii, consistent with the trend anticipated from anion

* Extrapolation of the Na curve gives $r({}^{\text{IV}}\text{Na}^+) = 0.90$ Å.

Fig. 3. Typical bond length *vs* bond strength plot.

repulsion effects. A similar comparison with Fe^{2+} and Ni^{2+} cannot be made because of electron distribution changes from tetrahedral to square planar coordination.

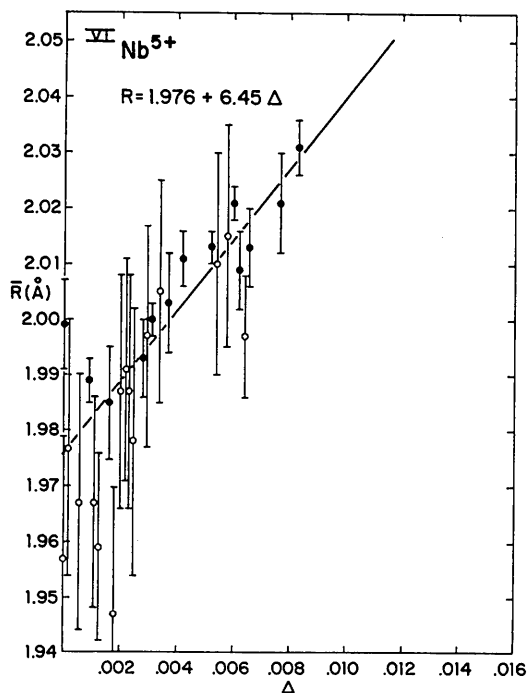


Fig. 4. Mean Nb^{5+} -O bond length vs distortion. Vertical bars represent average e.s.d.'s quoted by the authors. Solid circles represent more accurate data.

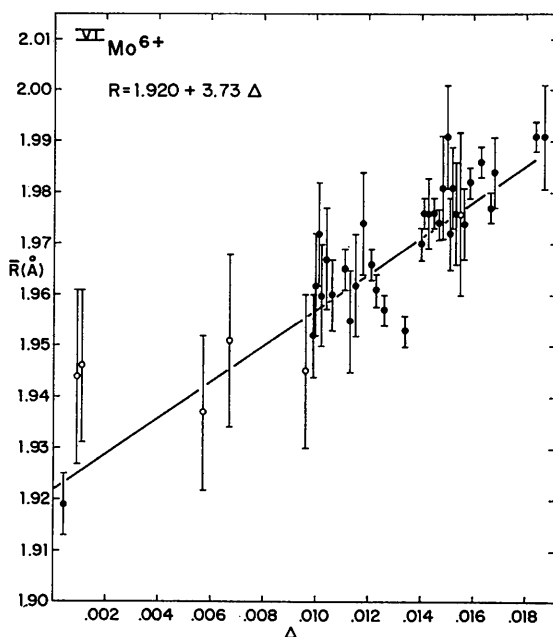


Fig. 5. Mean Mo^{6+} -O bond length vs distortion.

Table 4. Interatomic distances in some compounds containing tetrahedral and octahedral Na^+

Compound	\bar{R} (Å)	r (Å)	Reference
(a) IV Na^+			
Na_2O	2.40	1.02	
$\text{Na}_5\text{P}_3\text{O}_{10}$	2.37	0.99	60 ACCRA 13 263
$\text{NaOH} \cdot \text{H}_2\text{O}$	2.36	1.00	57 ACCRA 10 462
Na_6ZnO_4	2.39	0.99	69 ZAACA409 69
Mean	2.38	1.00	
(b) VI Na^+			
Na_2WO_4	2.38	1.00	74 ACBCA 30 1872
$\text{NaC}_6\text{O}_7\text{H}_7$	2.37	1.01	65 ACCRA 19 561
$\text{Na}_4\text{Sn}_2\text{Ge}_4\text{O}_{12}(\text{OH})_4$	2.39	1.02	70 ACSAA 24 1287
$\text{Na}_2\text{P}_2\text{O}_7 \cdot 10\text{H}_2\text{O}$	2.48	1.10	64 ACCRA 17 672
NaHCO_3	2.44	1.06	65 ACCRA 18 818
$\text{Na}_2\text{B}_4\text{O}_6(\text{OH})_2 \cdot 3\text{H}_2\text{O}$	2.41	1.04	67 SCIEA 154 1453
$\text{Na}_4\text{P}_4\text{O}_{12} \cdot 4\text{H}_2\text{O}$	2.415	1.05	61 ACCRA 14 555
$\text{NaAl}(\text{SO}_4)_2 \cdot 12\text{H}_2\text{O}$	2.45	1.10	67 ACCRA 22 182
$\text{NaB}(\text{OH})_4 \cdot 2\text{H}_2\text{O}$	2.460	1.09	63 ACCRA 16 1233
NaU acetate	2.375	1.025	59 ACCRA 12 526
$\text{C}_{10}\text{H}_{13}\text{N}_5\text{NaO}_6\text{P} \cdot 6\text{H}_2\text{O}$	2.406	1.046	75 ACBCA 31 19
Mean	2.42	1.05	

Factors affecting mean interatomic distances

Additivity of radii to give mean interatomic distances is not so important to the synthetic chemist who is primarily interested in ionic radii for predicting substitution in crystal structures. Crystallographers and physicists, however, are concerned with comparing calculated and experimental interatomic distances and predicting distances, e.g. for distance least-squares (DLS) structure refinements (Baur, 1972; Tillmanns, Gebert & Baur, 1973; Dempsey & Strens, 1975). The effective ionic radii in Table 1 can be used to reproduce moderately well most average interatomic distances in oxides and fluorides. However, certain deviations do occur. Some of these are unexplained but others can be attributed to (1) polyhedral distortion, (2) covalence, (3) partial occupancy of cation sites, or (4) electron delocalization.

1. Polyhedral distortion

To see the effects of polyhedral distortion consider the relationship between bond length (R) and Pauling bond strength (s) (Brown & Shannon, 1973). The analytical expression $s = s_0(R/R_0)^{-N}$, where s_0 is an ideal bond strength associated with R_0 , and R_0 and N are fitted parameters, was evaluated for cation-oxygen pairs for the first three rows of the periodic table. Using these relationships, the sums of bond strengths about cations and anions were found to equal the valences with a mean deviation of about 5%. Accepting the approximate validity of Pauling's second rule, $p = \sum s$ where $p = \text{valence}$, it is possible to derive the effects of distortion of various polyhedra on their mean bond distances. Fig. 3 shows a typical R - s curve. An undistorted octahedron results in an average bond strength \bar{s} and a mean distance \bar{R}_1 . A distorted octahedron with three bonds of length R_a and three of length R_b results in the same average bond strength, \bar{s} , but a mean distance $\bar{R}_2 > \bar{R}_1$.

The effects of distortion on mean bond lengths in numerous polyhedra have been determined. Although distortions in tetrahedra are not as important as in octahedra, they can contribute to variations in mean tetrahedral distances (Baur, 1974; Hawthorne, 1973). Strongly distorted octahedra like those containing V^{5+} , Cu^{2+} , and Mn^{3+} show a significant variation in mean distance with distortion, Δ^* (Brown & Shannon, 1973; Shannon & Calvo, 1973a; Shannon, Gumerman & Chenavas, 1975). Octahedra containing Mg^{2+} , Zn^{2+} , Co^{2+} , and Li^+ are generally less distorted than those of V^{5+} , Cu^{2+} , and Mn^{3+} and show a less pronounced dependence on mean bond length (Brown & Shannon, 1973).

The effects of distortion on mean bond lengths in $Nb^{5+}-O$ and $Mo^{6+}-O$ octahedra are illustrated in Figs. 4 and 5. Tables 5 and 6 list the data used to derive the figures.

Table 7 lists the results of linear regression analyses of mean bond length on distortion for all octahedra studied. It is clear from Fig. 4 that undistorted Nb^{5+} octahedra in pyrochlores have a distinctly smaller mean value than in compounds like $NbOPO_4$, $CaNb_2O_6$, and Na_3NbO_4 . Most of the accurately refined molybdates have relatively distorted octahedra. However, certain ordered perovskites with no octahedral distortion such as Ba_2CaMoO_6 would be expected to have much smaller mean $Mo^{6+}-O$ distances than a typical molyb-

date. In fact, the $Mo^{6+}-O$ octahedra in $Mo_2(O_2C_6Cl_4)_6$ with a very small distortion have the short mean distance of 1.919 Å.

Table 7 also lists the results of regression analyses for $Ta^{5+}-O$ and $W^{6+}-O$ octahedra but they are only approximate because of the scarcity of accurate structural data. Analysis of $Ti^{4+}-O$ octahedra was unsuccessful because of scatter in the data. Distances in $Ba_6Ti_{17}O_{40}$ (Tillmanns & Baur, 1970) and $BaTiO_3$ (Evans, 1951) deviated significantly from a linear relation.

Relations between mean distance and distortion should be particularly useful to help determine oxidation states in mixed valence compounds with such combinations as $Mo^{5+}-Mo^{6+}$, $W^{5+}-W^{6+}$, $V^{4+}-V^{5+}$, $Nb^{4+}-Nb^{5+}$ and $Mn^{3+}-Mn^{4+}$. Such considerations helped rationalize $Mn-O$ distances in $NaMn_7O_{12}$ and the mineral pinakiolite (Shannon, Gumerman & Chenavas, 1975).

The radii in Table 1 are generally derived for an average degree of distortion. Thus, interatomic distances calculated from these radii may be inaccurate if the distortion in a particular compound is much less or greater than usual. This applies particularly to cations whose polyhedra frequently show a large distortion, e.g. Mo^{6+} , Nb^{5+} , V^{5+} , Ba^{2+} , and the alkali ions.

2. Effects of partial occupancy of cation sites on mean cation-anion distances

In compounds with partially occupied sites, abnormally large cation-anion distances are usually found, as expected if the anions surrounding unoc-

* Octahedral distortion is defined by $\Delta = \frac{1}{6} \sum (R_i - \bar{R}) / \bar{R}$ where \bar{R} = average bond length and R_i = an individual bond length.

Table 5. Comparison of mean octahedral $Nb^{5+}-O$ distances with distortion

Only structures with e.s.d.'s for $Nb-O$ distances of < 0.025 Å were used.

Compound	\bar{R} (Å)	Distortion $\Delta = \langle (\Delta R/R)^2 \rangle \times 10^4$	Reference	
Hg ₂ Nb ₂ O ₇	1.999	0	68 INOCA	7 1704
Cd ₂ Nb ₂ O ₇	1.957	0	72 CJCHA	50 3648
Na ₂ Nb ₄ O ₁₁	1.977	1	70 JSSCB	1 454
Ba _{0.27} Sr _{0.75} Nb ₂ O _{5.78}	1.967	6	61 JCPSA	48 5048
Na ₁₃ Nb ₃₅ O ₉₄	1.965	7	71 JSSCB	3 89
Ba ₃ Si ₄ Nb ₆ O ₂₆	1.989	9	70 ACBCA	26 102
Na ₁₃ Nb ₃₅ O ₉₄	1.967	11	71 JSSCB	3 89
Na ₁₃ Nb ₃₅ O ₉₄	1.959	12	71 JSSCB	3 89
Na ₁₃ Nb ₃₅ O ₉₄	1.964	12	71 JSSCB	3 89
NaNbO ₃	1.985	16	69 ACBCA	25 851
Na ₁₃ Nb ₃₅ O ₉₄	1.947	18	71 JSSCB	3 89
Na ₁₃ Nb ₃₅ O ₉₄	1.991	22	71 JSSCB	3 89
Na ₁₃ Nb ₃₅ O ₉₄	1.987	22	71 JSSCB	3 89
Na ₁₃ Nb ₃₅ O ₉₄	1.978	24	71 JSSCB	3 89
LiNb ₅ O ₈	1.993	28	71 ACSAA	25 3337
LiNbO ₃	2.000	31	66 JPCSA	27 997
Ca ₂ Nb ₂ O ₇	1.997	31	74 JINCA	36 1965
Ca ₂ Nb ₂ O ₇	2.005	34	74 JINCA	36 1965
SbNbO ₄	2.003	37	65 CCJDA	1965 611
KNbO ₃	2.011	42	67 ACACA	22 639
Na ₃ NbO ₄	2.013	52	74 BUFGA	97 3
Ca ₂ Nb ₂ O ₇	2.010	53	74 JINCA	36 1965
Ca ₂ Nb ₂ O ₇	2.015	58	74 JINCA	36 1965
Na ₃ NbO ₄	2.021	60	74 BUFGA	97 3
CaNb ₂ O ₆	2.021	76	70 AMMIA	55 90
GaNbO ₄	2.031	83	65 ACACA	18 874

Table 6. Comparison of mean octahedral Mo⁶⁺-O distances with distortion

Only structures with e.s.d.'s for Mo-O distances of <0.025 Å were used.

Compound	\bar{R} (Å)	Distortion		Reference	
		$\Delta = \langle (\Delta R/R)^2 \rangle \times 10^4$			
Mo ₂ (O ₂ C ₆ Cl ₄) ₆	1.919	5	75 JACSA	97	2123
Mo ₄ O ₁₁ orthorhombic	1.944	9	63 ARKEA	21	365
Mo ₄ O ₁₁ monoclinic	1.946	10	63 ARKEA	21	365
Mo ₄ O ₁₁ monoclinic	1.937	56	63 ARKEA	21	365
Mo ₄ O ₁₁ orthorhombic	1.951	67	63 ARKEA	21	365
Mo ₄ O ₁₁ orthorhombic	1.911	96	63 ARKEA	21	365
Mo ₄ O ₁₁ monoclinic	1.945	96	63 ARKEA	21	365
(C ₁₅ H ₁₁ O ₂) ₂ MoO ₂	1.952	99	74 ACBCA	30	300
(NH ₄) ₆ [Mo ₇ O ₂₄]·4H ₂ O	1.962	99	75 JCSIA	1975	505
(NH ₄) ₆ [Mo ₇ O ₂₄]·4H ₂ O	1.972	101	75 JCSIA	1975	505
(NH ₄) ₆ [Mo ₇ O ₂₄]·4H ₂ O	1.960	104	75 JCSIA	1975	505
LiMoO ₂ AsO ₄	1.967	104	70 ACSAA	24	3711
(NH ₄) ₆ Mo ₈ O ₂₇ ·4H ₂ O	1.960	106	74 ACBCA	30	48
HgMoO ₄	1.965	111	73 ACBCA	29	869
(NH ₄) ₆ [Mo ₇ O ₂₄]·4H ₂ O	1.955	113	75 JCSIA	1975	505
(NH ₄) ₆ [Mo ₇ O ₂₄]·4H ₂ O	1.962	115	75 JCSIA	1975	505
(NH ₄) ₆ [Mo ₇ O ₂₄]·4H ₂ O	1.974	118	68 JACSA	90	3275
MoO ₃ ·2H ₂ O	1.966	121	72 ACBCA	28	2222
MoO ₃ ·2H ₂ O	1.961	123	72 ACBCA	28	2222
MoO ₃ ·2H ₂ O	1.957	126	72 ACBCA	28	2222
MoO ₃ ·2H ₂ O	1.953	134	72 ACBCA	28	2222
(NH ₄) ₅ [MoO ₃] ₅ (PO ₄)(HPO ₄)·3H ₂ O	1.970	140	74 JCSIA	1974	941
Na ₃ (CrMo ₆ O ₂₄ H ₆)·8H ₂ O	1.976	141	70 INOCA	9	2228
(NH ₄) ₆ Mo ₈ O ₂₇ ·4H ₂ O	1.976	141	74 ACBCA	30	48
Na ₃ CrMo ₆ O ₂₄ H ₆ ·8H ₂ O	1.976	143	70 INOCA	9	2228
(NH ₄) ₅ [(MoO ₃) ₅ (PO ₄)(HPO ₄)]·3H ₂ O	1.974	145	74 JCSIA	1974	941
(NH ₄) ₆ [TeMo ₆ O ₂₄]·Te(OH) ₆ ·7H ₂ O	1.981	147	74 ACBCA	30	2095
CoMoO ₄	1.991	150	65 ACACA	19	269
(NH ₄) ₆ Mo ₈ O ₂₇ ·4H ₂ O	1.972	151	74 ACBCA	30	48
MoO ₃	1.981	151	63 ARKEA	21	357
(NH ₄) ₆ [Mo ₇ O ₂₄]·4H ₂ O	1.976	152	68 JACSA	90	3275
K ₂ {[MoO ₂ (C ₂ O ₄)(H ₂ O)] ₂ O}	1.976	152	64 INOCA	3	1603
(NH ₄) ₆ Mo ₈ O ₂₇ ·4H ₂ O	1.974	152	74 ACBCA	30	48
(NH ₄) ₅ [(MoO ₃) ₅ (PO ₄)(HPO ₄)]·3H ₂ O	1.982	159	74 JCSIA	1974	941
Na ₃ CrMo ₆ O ₂₄ H ₆ ·8H ₂ O	1.986	163	70 INOCA	9	2228
(NH ₄) ₅ [(MoO ₃) ₅ (PO ₄)(HPO ₄)]·3H ₂ O	1.977	167	74 JCSIA	1974	941
MoO ₃ ·H ₂ O	1.984	167	74 ACBCA	30	1795
(NH ₄) ₅ [(MoO ₃) ₅ (PO ₄)(HPO ₄)]·3H ₂ O	1.991	186	74 JCSIA	1974	941
(NH ₄) ₆ [Mo ₇ O ₂₄]·4H ₂ O	1.991	189	75 JCSIA	1975	505
(NH ₄) ₆ [Mo ₇ O ₂₄]·4H ₂ O	2.008	197	75 JCSIA	1975	505

Table 7. Variation of mean M-O distance and effective ionic radius in octahedral environments as a function of distortion

Ion	Maximum $\Delta \times 10^4$	N*	R ₀ †	r ₀ ‡	m	Correlation coefficient	Goodness of fit (× 10 ³)
Mo ⁶⁺	212	38	1.920		3.73	0.74	67
				0.572	3.01	0.63	70
W ⁶⁺	122	7	1.925		3.30	0.75	19
				0.565	3.28	0.66	24
V ⁵⁺	576	16	1.887		2.62	0.98	8
Nb ⁵⁺	83	29	1.976		6.45	0.69	71
				0.599	6.83	0.44	99
Ta ⁵⁺	79	6	1.984		6.70	0.81	18
				0.617	3.79	0.15	46
Mn ³⁺	71	15	1.994		7.08	0.82	30
				0.624	6.15	0.54	50
Cu ²⁺	316	26	2.085		3.99	0.82	77
Mg ²⁺	156	28	2.094		8.31	0.72	21
				0.728	8.86	0.77	18
Co ²⁺	46	15	2.106		7.38	0.42	19
				0.734	11.70	0.70	16
Zn ²⁺	71	16	2.099		7.70	0.64	21
				0.736	8.20	0.74	16
Li ⁺	148	11	2.159		8.42	0.81	30
				0.784	9.02	0.79	35

* N = number of independent octahedra

† R = R₀ + mΔ.‡ r = r₀ + mΔ.

cupied sites relax toward their bonded cation neighbors. Therefore average distances should increase as the occupancy factor decreases. In general, partial occupancy seems to be more prevalent for cations which are weakly bonded to oxygen like Cu^+ , Ag^+ , alkali ions, and large alkaline earths. The most prominent examples are Li and Na compounds. Table 8 summarizes the existent data on some structures with partial cation occupancy. Fig. 6 shows the dependence of mean Li–O bond length on the degree of occupancy. Although the data are not extensive, it is apparent that mean distance increases as occupancy factor decreases. Extrapolation of the Li curve in Fig. 6 to zero occupancy, *i.e.* a tetrahedral Li vacancy, gives 2.10–2.15 Å, which is close to the 2.11 Å found for $\alpha\text{-Li}_5\text{GaO}_4$ by Stewner & Hoppe (1971) and for β eucryptite by Tscherry, Schulz & Laves (1972).

Another example of the effects of partial occupancy can be found in the non-stoichiometric feldspar $\text{Sr}_{0.84}\text{Na}_{0.03}\text{Al}_{1.69}\text{Si}_{2.29}\text{O}_8$ reported by Grundy & Ito (1974). The mean Sr–O distance in this compound is 0.03 Å greater than in the stoichiometric $\text{SrAl}_2\text{Si}_2\text{O}_8$ (Chiari, Calleri, Bruno & Ribbe, 1975).

The relation between mean distance and occupancy probably cannot be quantified precisely because the relaxation of oxygen ions will depend on the nature and number of other cation neighbors.

3. Effects of covalence

Changes in interatomic distances due to covalence effects are anticipated in compounds with (1) anions less electronegative than fluorine or oxygen, *i.e.* chlor-

ides, bromides, sulfides, selenides, *etc.* and (2) tetrahedral oxyanions such as the VO_4^{3-} and AsO_4^{3-} groups. The effects of covalence show up as a lack of additivity of the radii and are generally referred to as ‘covalent shortening’.

(a) *Halides and chalcogenides.* Covalence effects can be observed by comparing the relative contraction of cation–anion distances in two different isotypic compounds as the anion becomes less electronegative, *e.g.* Fe^{2+} in Fe_2GeO_4 and Fe_2GeS_4 vs Mg^{2+} in Mg_2GeO_4 and Mg_2GeS_4 . Covalence shortens both Fe–S and Mg–S bonds relative to Fe–O and Mg–O bonds, but because of the greater electronegativity of Fe^{2+} (1.8) compared to Mg^{2+} (1.2), the Fe–S bonds are shortened to a greater extent. Thus a ‘covalency contraction’ parameter (Shannon & Vincent, 1974) can be defined:

$$R_d = \frac{d(\text{Fe-X})^3}{d(\text{Mg-X})^3}$$

where $d(\text{Fe-X})$ = mean Fe–X distance.

A similar parameter

$$R_v = \frac{V(\text{Fe}_m\text{X}_n)}{V(\text{Mg}_m\text{X}_n)}$$

compares the volume of an Fe^{2+} compound with that of an isotypic Mg^{2+} compound. To see the effects of covalence on the Fe–X distance relative to the Mg–X distance, the ratio R_v or R_d may be plotted against the difference in electronegativity of the Fe–X bond, $\Delta\chi_{\text{Fe-X}}$. Such schematic R_v – $\Delta\chi$ plots are shown in Fig. 7. The reference ions for Cd^{2+} and In^{3+} are Ca^{2+} and Sc^{3+} respectively. Such plots usually show a strong

Table 8. Mean distances in structures with partially occupied cation sites

Compound	Occupancy factor	\bar{R}	Reference		
(a) IVLi^+					
Typical	1.00	1.97	Table 1		
LiAlSiO_4 (β eucryptite)	1.00	2.020 (4)	73 AMMIA	58	681
		2.025 (7)	72 ZKKKA	135	175
$\text{LiAlSi}_2\text{O}_6$ II (β spodumene)	0.50	2.08 (4)	68 ZKKKA	126	46
		2.085 (9)	69 ZKKKA	130	420
LiAlSiO_4 (β eucryptite)	0.50	2.056 (2)	72 ZKKKA	135	161
$\text{Li}_2\text{Al}_2\text{Si}_3\text{O}_{10}$	0.40	2.064 (4)	70 ZKKKA	132	118
$\text{LiAlSi}_2\text{O}_6$ III	0.33	2.068 (5)	68 ZKKKA	127	327
$\alpha\text{-Li}_5\text{GaO}_4$	0.00	2.11	71 ACBCA	27	616
LiAlSiO_4	0.00	2.11	72 ZKKKA	135	175
(b) VNa^+					
Typical	1.00	2.42	Table 1		
$\text{Na}_2\text{Fe}_2\text{Al}(\text{PO}_4)_3$ (wylieite)	0.91	2.533 (6)	74 AMMIA	59	280
NaSbO_3	0.82	2.74	74 JSSCB	9	345
$\text{Na}_2\text{Fe}_2\text{Al}(\text{PO}_4)_3$ (wylieite)	0.70	2.723 (6)	74 AMMIA	59	280
$\text{NaAlSi}_3\text{O}_8$ (high albite)	0.50	2.600 (9)	69 ACBCA	25	1503
$\text{NaAl}_{11}\text{O}_{17}$ ($\beta\text{-Al}_2\text{O}_3$)	0.35	2.839 (1)	68 ZKKKA	127	94
NaSbO_3	0.29	2.65	74 JSSCB	9	345
$\text{Na}_{2.58}\text{Al}_{21.81}\text{O}_{34}$ ($\beta\text{-Al}_2\text{O}_3$)	0.25	2.88	71 ACBCA	27	1826
(c) VAg^+					
Typical	1.00	2.50	Table 1		
AgSbO_3	0.44	2.64	74 JSSCB	9	345
AgSbO_3	0.33	2.75	74 JSSCB	9	345
$\text{Ag}_{2.4}\text{Al}_{22}\text{O}_{34.2}$	0.22	2.83	72 JSSCB	4	60

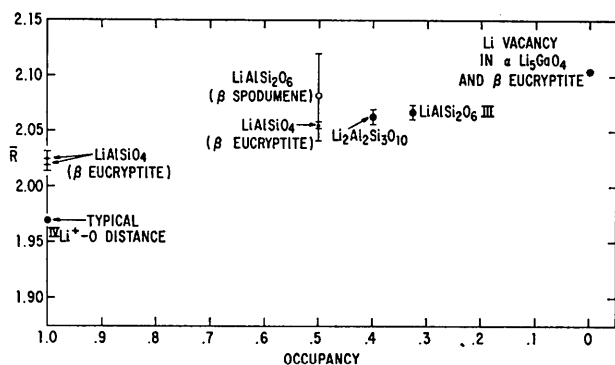


Fig. 6. Mean $\text{Li}^+\text{-O}$ bond length vs partial occupancy.

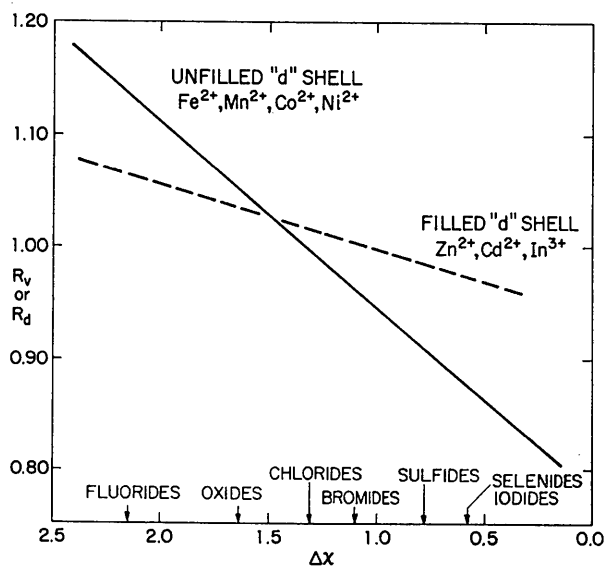


Fig. 7. Covalency contraction parameter, R_v or R_d , vs $\Delta\chi$ for filled and unfilled d shell cations.

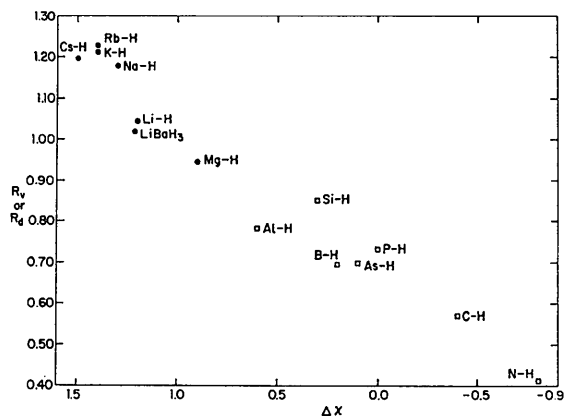


Fig. 8. Covalency contraction parameter, R_v or R_d , vs $\Delta\chi$ for hydrides. Solid circles represent ratios of cell volumes of isotopic compounds. Squares represent ratios of the cubed M-H distances to the cubed M-F distances.

dependence of R_v on $\Delta\chi$. For $\text{Fe}^{2+}\text{-Mg}^{2+}$ the Fe^{2+} fluoride volumes are $\sim 110\%$ of the corresponding Mg^{2+} fluoride volumes whereas the Fe^{2+} sulfide volumes are $\sim 96\%$ of the corresponding Mg^{2+} sulfide volumes. Plots for the cations with filled ' d ' shells show a markedly smaller dependence on $\Delta\chi$. This appears to be due to the difference in covalence of hybrid orbitals formed from metal ' d ' orbitals vs metal ' $s-p$ ' orbitals.

These relations show that effective ionic radii derived primarily from oxides are not strictly applicable to fluorides – note the change in R_v for Fe^{2+} , Co^{2+} , Ni^{2+} , and Mn^{2+} from fluorides to oxides. This effect is particularly noticeable in $R_v\text{-}\Delta\chi$ plots for the pairs $\text{Cu}^+\text{-Li}^+$ and $\text{Ag}^+\text{-Na}^+$ (Shannon & Gummerman, 1975). The $\text{Cu}^+\text{-Li}^+$ and $\text{Ag}^+\text{-Na}^+$ plots are very steep, e.g. the volume of AgF is 120% of the volume of NaF , whereas the volume of Ag_2Se is only 72% of the volume of Na_2Se . Although most of this change arises from covalency, double repulsion effects present in the Li and Na halides described by Pauling (1960) may also play a role.

Covalence effects are useful in explaining certain differences between the effective ionic radii of Table 1 and the ionic radii of Pauling (1927) and Ahrens (1952). Pauling's radii for Cu^+ (0.96 Å) and Ag^+ (1.26 Å) are considerably larger than those in Table 1 (0.77 and 1.15 Å respectively). Since these radii were derived from comparison of alkali halide distances, using an equation relating effective nuclear charge and screening constants (Pauling, 1927), they are valid in primarily ionic crystals. The smaller radii in Table 1 are applicable in the more covalent oxides. Extrapolation of R vs $\Delta\chi$ curves such as in Fig. 7 leads to values of 0.91 Å and 1.23 Å for fluorides, which are close to Pauling's ionic values.

A final example of covalence effects concerns $\text{M}^+\text{-H}^-$ distances. According to Gibb (1962), the radius of the hydride ion is slightly larger than the radius of the fluoride ion. To rationalize the behavior of the hydride ion, the M-H bond has been treated as covalent. Therefore, it is useful to make R_v vs $\Delta\chi$ plots similar to those just discussed for Fe^{2+} , Cu^+ , etc. In this case, the reference ion is F^- and volumes of certain hydrides are compared to those of isotopic fluorides. The results of this analysis are shown in Fig. 8. The solid circles represent volume ratios, $R_v = V(\text{M}_m\text{H}_n)/V(\text{M}_m\text{F}_n)$; open squares represent ratios of typical distances $R_d = d(\text{M-H})^3/d(\text{M-F})^3$. In the more ionic hydrides of Cs, Rb, K, and Na, hydride volumes are considerably larger than those of the fluorides. For the Li and Mg compounds, hydride and fluoride volumes are approximately equal, whereas the more covalent hydrides have increasingly smaller relative volumes than the corresponding fluorides. Fig. 8 partly explains the differences in reported radii. The Morris & Reed (1965) value of 1.53 Å was derived essentially from the large alkali halides, while Gibb's value of 1.40 Å was derived primarily from hydrides of the more electronegative

metals such as: Sc, Ti, Y, Zr, Hf, Nb, Ta, and Th. Because of this strong dependence of M–H distances on cation electronegativity, it does not seem very useful to quote a unique radius for H^- .

(b) *Tetrahedral oxyanions.* Lack of additivity also appears in most small tetrahedral groups and is particularly noticeable for the ions $^{IV}B^{3+}$, $^{IV}Fe^{3+}$, $^{IV}Ge^{4+}$, $^{IV}As^{5+}$, $^{IV}V^{5+}$, $^{IV}S^{6+}$, $^{IV}Se^{6+}$, and $^{IV}Cl^{7+}$. The deviations in vanadates have been studied in detail (Shannon & Calvo, 1973*b*). Assuming that the V–O bond is strongly covalent, and that relatively electronegative cations such as Cu^{2+} , Ni^{2+} , and Co^{2+} tend to remove electron density from the V–O bond, a V–O bond length increase in Cu, Ni, and Co vanadates is anticipated. Plots of mean radii (\bar{r}) vs mean cation electronegativity ($\bar{\chi}$) show a marked slope with a gradual increase in $\bar{r}(^{IV}V^{5+})$ from vanadates of the alkali and alkaline earth ions to those of Cu, Ni, and Co. Similar plots for other ions, P^{5+} , As^{5+} (Shannon & Calvo, 1973*b*), B^{3+} , Si^{4+} , Se^{6+} (Shannon, 1975), showed the same behavior. The statistical data on the tetrahedra of B^{3+} , Si^{4+} , Ge^{4+} , P^{5+} , As^{5+} , S^{6+} , Se^{6+} , Cr^{6+} , Mo^{6+} , W^{6+} , and Cl^{7+} have been summarized by Shannon (1975). The slopes of the \bar{r} vs $\bar{\chi}$ plots were greatest for V^{5+} , Se^{6+} , and Cl^{7+} , and least for Si^{4+} . Although the evidence for covalence as the origin of these effects in the above systems is only indirect, this behavior is consistent with accepted ideas of ‘covalent shortening’ of bonds.

The evidence for covalent shortening of $^{IV}Fe^{3+}$ –O bonds is more direct. Jeitschko, Sleight, McClellan & Weiher (1976) have found a good correlation between (1) the Fe Mössbauer isomer shift and mean Fe–O distance and (2) $\bar{\chi}$ and mean Fe–O distance (\bar{R}). Thus, in β - $NaFeO_2$ $\bar{R}=1.86$ Å and $\delta=0.18$ mm s^{-1} relative to α Fe whereas in $Bi_3(FeO_4)(MoO_4)_2$ $\bar{R}=1.909$ Å and $\delta=0.282$ mm s^{-1} .

4. Effects of electron delocalization

At a pressure of 6.5 kbar SmS (NaCl structure) undergoes a semiconductor to metal transition and a reduction in cell edge from 5.97 to 5.70 Å (Jayaraman, Narayanamurti, Bucher & Maines, 1970). The reduction in cell volume was attributed to a partial conversion of Sm^{2+} to Sm^{3+} ; some of the electrons presumably go into a conduction band.

Electron delocalization effects can also be seen by comparing the volumes of the conducting V sulfides VS, V_7S_8 , V_3S_4 and V_5S_8 with the corresponding Cr sulfides which have localized ‘*d*’ electrons (de Vries & Jellinek, 1974). The V compounds have volumes ~5% smaller than the corresponding chromium compounds. This does not agree with the relative sizes of V and Cr in oxides and fluorides, e.g. $r(^{IV}V^{3+})=0.64$ and $r(^{VI}Cr^{3+})=0.615$ Å. For the sulfides, this unit-cell volume anomaly is not simply attributable to metallic vs semiconducting behavior. While Cr_3S_4 , Cr_5S_6 , and Cr_7S_8 show a positive temperature dependence of resistivity typical of a metal, magnetic susceptibility

measurements indicate Curie–Weiss behavior and therefore nearly localized electrons (van Bruggen, 1969). This is in contrast to the Pauli paramagnetic behavior of the corresponding V sulfides (de Vries & Haas, 1973) characteristic of delocalized electrons. Thus, in SmS and the sulfides of V metallic character accompanied by electron delocalization appears to be associated with reduced bond distances.

A further example of delocalization effects occurs in the compound $NaVS_2$ (Weigers, van der Meer, van Heinigen, Kloosterboer & Alberink, 1974). The molecular volume of Pauli paramagnetic $NaVS_2$ I (67.9 Å³) is significantly less than that of $NaVS_2$ II (72.7 Å³). $NaVS_2$ II is characterized by localized electrons (Jellinek, 1975) and its molecular volume is consistent with that of isotopic $NaCrS_2$ (71.1 Å³).

If electron delocalization in oxides results in reduced metal–oxygen distances and thereby an effective increase in valence, radii derived for the ions Mo^{4+} , Tc^{4+} , Ru^{4+} , Rh^{4+} , W^{4+} , Re^{4+} , Os^{4+} , and Ir^{5+} from metallic oxides may not be reliable when applied to insulating oxides. Thus, radii obtained from distances in the metallic phases, e.g. RhO_2 , ReO_2 , and $Cd_2Ir_2O_7$, will be smaller than radii obtained from semiconducting or insulating compounds.* When both types of compounds have been studied, a significant difference in distances is generally found. The mean octahedral Re^{4+} –O distance in insulating $K_4[Re_2O_2(C_2O_4)_4] \cdot 3H_2O$ (Lis, 1975) of 2.021 (10) Å ($r=0.671$ Å) is greater than the estimated mean distance in metallic ReO_2 of 1.99 Å ($r=0.63$ Å). Knop & Carlow’s (1974) value of $r=0.662$ Å derived from cell volumes of the insulating Cs_2ReF_6 phases is consistent with the radius of Re^{4+} from $K_4[Re_2O_2(C_2O_4)_4] \cdot 3H_2O$. The Re^{5+} –O distance in $Nd_4Re_2O_{11}$ (Wilhelmi, Lagervall & Muller, 1970) of 1.987 (12) Å ($r=0.607$ Å) is significantly greater than the distance in metallic $Cd_2Re_2O_7$ (Sleight, 1975) of 1.93 (2) Å ($r=0.55$ Å). The radii of 0.58 Å derived from XeF_2RuF_6 and 0.60 Å from $XeFRuF_6$ (Bartlett, Gennis, Gibler, Morrell & Zalkin, 1973) are greater than the radius of 0.565 Å derived from the r^3 – V plot for metallic $Cd_2Ru_2O_7$. In contrast, however, the Mo^{4+} radius of 0.64 Å derived from insulating Li_2MoF_6 (Brunton, 1971) is not greatly different from the radius of 0.65 Å derived from metallic MoO_2 (Brandt & Skapski, 1967).

Although there appears to be ample evidence to show that M–O bond distances in compounds with localized electrons are greater than M–O distances in compounds with delocalized electrons, the data are not yet sufficient to derive a reliable set of radii for semiconducting compounds containing Mo^{4+} , Tc^{4+} , Ru^{4+} , Rh^{4+} , W^{4+} , Re^{4+} , Os^{4+} , and Ir^{5+} . This will become possible as additional accurate structure refinements of fluorides, molecular inorganic compounds, and semiconducting oxides containing these ions become available.

* This assumes that metallic character can be equated with delocalized electron behavior in these compounds.

I would like to acknowledge the help of F. Jelinek for providing unpublished data on NaVS_2 , F. C. Hawthorne for pointing out numerous structures containing partially occupied cation sites, O. Muller for several sources of radii of unusual ions, M. Fouassier for unpublished data on K_4MO_4 compounds, I. D. Brown for unpublished bond length-bond strength curves, and P. S. Gumerman for assistance with data collection. Structure data on rare earth halides and an analysis of the radii of divalent rare earths provided by H. Bärnighausen were especially valuable. I am particularly indebted to Ruth Shannon for the tabulation of data and proof reading. Finally, I would like to thank R. J. Bouchard, W. H. Baur, and H. Bärnighausen for critically reviewing the manuscript prior to publication.

References

- AHRENS, L. H. (1952). *Geochim. Cosmochim. Acta*, **2**, 155-169.
- BARTLETT, N., GENNIS, M., GIBLER, D., MORRELL, B. & ZALKIN, A. (1973). *Inorg. Chem.* **12**, 1717-1721.
- BAUR, W. H. (1972). *Amer. Min.* **57**, 709-731.
- BAUR, W. H. (1974). *Acta Cryst.* **B30**, 1195-1215.
- BIRCHALL, T. & SLEIGHT, A. W. (1975). *J. Solid State Chem.* **13**, 118-130.
- BONAMICO, M., DESSY, G., FARES, V. & SCARAMUZZA, L. (1974). *J. Chem. Soc. Dalton*, pp. 1258-1263.
- BRANDT, B. G. & SKAPSKI, A. C. (1967). *Acta Chem. Scand.* **21**, 661-667.
- BROWN, I. D. (1975). Private communication.
- BROWN, I. D. & SHANNON, R. D. (1973). *Acta Cryst.* **A29**, 266-282.
- BRUGGEN, C. F. VAN (1969). Ph.D. Thesis, Univ. of Groningen.
- BRUNTON, G. (1971). *Mater. Res. Bull.* **6**, 555-560.
- CHIARI, G., CALLERI, M., BRUNO, E. & RIBBE, P. H. (1975). *Amer. Min.* **60**, 111-119.
- Codens for Periodical Titles* (1966). Vol. II. ASTM Data series DS23A, Philadelphia.
- DEMPSEY, M. J. & STRENS, R. G. J. (1975). Proc. NATO Conf. on Petrophysics, Newcastle-upon-Tyne, April 22-26.
- EVANS, H. T. JR (1951). *Acta Cryst.* **4**, 377.
- FLYGARE, W. H. & HUGGINS, R. A. (1973). *J. Phys. Chem. Solids*, **34**, 1199-1204.
- FUKUNAGA, O. & FUJITA, T. (1973). *J. Solid State Chem.* **8**, 331-338.
- FUMI, F. G. & TOSI, M. P. (1964). *J. Phys. Chem. Solids*, **25**, 31-43.
- GELLER, S., WILLIAMS, H. J., ESPINOSA, G. P., SHERWOOD, R. C. & GILLO, M. A. (1963). *Appl. Phys. Lett.* **3**, 21-22.
- GIBB, T. R. P. (1962). *Prog. Inorg. Chem.* **3**, 315-509.
- GREIS, O. & PETZEL, T. (1974). *Z. anorg. allgem. Chem.* **403**, 1-22.
- GRUNDY, H. D. & ITO, J. (1974). *Amer. Min.* **59**, 1319-1326.
- HAWTHORNE, F. C. (1973). *The Crystal Chemistry of the Clino-Amphiboles*, Ph.D. Thesis, McMaster Univ.
- JAYARAMAN, A., NARAYANAMURTI, V., BUCHER, E. & MAINES, R. G. (1970). *Phys. Rev. Lett.* **25**, 1430-1433.
- JEITSCHKO, W., SLEIGHT, A. W., MCCLELLAN, W. R. & WEIHER, J. F. (1976). *Acta Cryst.* **B32**, 1163-1170.
- JELLINEK, F. (1975). Private communication.
- KÁLMÁN, A. (1971). *Chem. Commun.* pp. 1857-1859.
- KHAN, A. A. & BAUR, W. (1972). *Acta Cryst.* **B28**, 683-693.
- KNOP, O. & CARLOW, J. S. (1974). *Canad. J. Chem.* **52**, 2175-2183.
- LIS, T. (1975). *Acta Cryst.* **B31**, 1594-1597.
- MCCARTHY, G. J. (1971). *Mater. Res. Bull.* **6**, 31-40.
- MORRIS, D. F. C. & REED, G. L. (1965). *J. Inorg. Nucl. Chem.* **27**, 1715-1717.
- MULLER, O. & ROY, R. (1974). *Crystal Chemistry of Non-Metallic Materials. 4. The Major Ternary Structural Families*. New York: Springer-Verlag.
- PAULING, L. (1927). *J. Amer. Chem. Soc.* **49**, 765-794.
- PAULING, L. (1960). *The Nature of the Chemical Bond*. Ithaca: Cornell Univ. Press.
- PETERSON, J. R. & CUNNINGHAM, B. B. (1967). *Inorg. Nucl. Chem. Lett.* **3**, 327-336.
- PETERSON, J. R. & CUNNINGHAM, B. B. (1968). *J. Inorg. Nucl. Chem.* **30**, 1775-1781.
- RIBBE, P. & GIBBS, G. V. (1971). *Amer. Min.* **56**, 1155-1173.
- SHANNON, R. D. (1975). Proc. NATO Conf. on Petrophysics, Newcastle-upon-Tyne, April 22-26.
- SHANNON, R. D. & CALVO, C. (1973a). *Acta Cryst.* **B29**, 1338-1345.
- SHANNON, R. D. & CALVO, C. (1973b). *J. Solid State Chem.* **6**, 538-549.
- SHANNON, R. D. & GUMERMAN, P. S. (1975). *J. Inorg. Nucl. Chem.* **38**, 699-703.
- SHANNON, R. D., GUMERMAN, P. S. & CHENAVAS, J. (1975). *Amer. Min.* **60**, 714-716.
- SHANNON, R. D. & PREWITT, C. T. (1969). *Acta Cryst.* **B25**, 925-945.
- SHANNON, R. D. & VINCENT, H. (1974). *Struct. Bond. (Berlin)*, **19**, 1-43.
- SILVA, R. J., MCDOWELL, W. J., KELLER, O. L. & TARRANT, J. R. (1974). *Inorg. Chem.* **13**, 2233-2237.
- SLEIGHT, A. W. (1975). Private communication.
- SLEIGHT, A. W. & JONES, G. (1975). *Acta Cryst.* **B31**, 2748-2749.
- STEWART, D., KNOP, O., MEADS, R. & PARKER, W. (1973). *Canad. J. Chem.* **51**, 1041-1049.
- STEWNER, F. & HOPPE, R. (1971). *Acta Cryst.* **B27**, 616-621.
- TILLMANN, E. & BAUR, W. H. (1970). *Acta Cryst.* **B26**, 1645-1654.
- TILLMANN, E., GEBERT, W. & BAUR, W. H. (1973). *J. Solid State Chem.* **7**, 69-84.
- TSCHERRY, V., SCHULZ, H., & LAVES, F. (1972). *Z. Kristallogr.* **135**, 175-198.
- VRIES, A. B. DE & HAAS, C. (1973). *J. Phys. Chem. Solids*, **34**, 651-659.
- VRIES, A. B. DE & JELLINEK, F. (1974). *Rev. Chim. Miner.* **11**, 624-636.
- WEIGERS, G., VAN DER MEER, R., VAN HEININGEN, H., KLOOSTERBOER, H. & ALBERINK, A. (1974). *Mater. Res. Bull.* **9**, 1261-1266.
- WILHELMI, K., LAGERVALL, E. & MULLER, O. (1970). *Acta Chem. Scand.* **24**, 3406-3408.
- WOLFE, R. W. & NEWNHAM, R. E. (1969). *J. Electrochem. Soc.* **116**, 832-835.